Journal of Catalyst & Catalysis
E-ISSN:2349-4344
Volume- 13 Issue- 01 Year- 2026
Review Article
Received Date: April 18, 2026
Accepted Date: April 20, 2026
Published Date: April 30, 2026

Catalyst-Driven Degradation and Failure Analysis of Intergranular Cracking in 316H Studded Pipes under Refinery Heat Recovery Conditions

***Urvesh Vala*[1*], *Anunad Mishra*[2]**

[*1]*Head, Material Engineering & Technology, L&T Energy Hydrocarbon Engineering Limited, Vadodara, Gujarat, India*

[2]*Engineer, Material Engineering Technology, L&T Energy Hydrocarbon Engineering Limited, Vadodara, Gujarat, India*

Corresponding Email: urvesh.vala@larsentoubro.com

Abstract

A failure analysis investigation was carried out on a high-temperature studded pipe used in a convection module for heat recovery in an oil and gas refinery application after leakage was detected during pre-commissioning hydrotesting. The investigated pipe was manufactured from AISI 316H austenitic stainless steel, and carbon steel studs had been joined to its outer surface by high-frequency resistance welding. Two leaks were reported in the pipe under investigation, and a sample containing one leaking region was removed for detailed examination. The failed sample was examined by visual inspection, dye penetrant testing, optical emission spectroscopy, stereomicroscopy, metallographic sectioning, scanning electron microscopy, and energy-dispersive spectroscopy. The leak was associated with a longitudinal crack that propagated through the pipe wall thickness and exhibited a predominantly intergranular morphology. Metallographic examination further showed that one end of the crack was located at a lack-of-fusion region between the stud and the external surface of the

pipe. Localized bulging and heat tint were also observed in the damaged zone. A copperish-colored matter was observed along the crack surfaces during optical examination, and EDS analysis later confirmed the presence of copper both on the opened fracture surface and along the internal crack surfaces in cross-section. Based on the combined metallographic, fractographic, and elemental evidence, the failure was attributed to an intergranular decohesion mechanism consistent with liquid metal embrittlement of austenitic stainless steel by copper during the stud welding stage, likely assisted by local overheating. Further investigation into the source and transfer route of copper contamination was strongly recommended.

Keywords

AISI 316H; studded pipe; hydrotest leakage; intergranular cracking; copper contamination; liquid metal embrittlement; SEM; EDS; failure analysis.

1. Introduction

Studded piping is used in convection modules for heat recovery in oil and gas refinery applications, where structural integrity and fabrication quality are critical to safe operation. In the present case, leakage was detected during hydrotesting of a high-temperature studded pipe prior to commissioning. Since hydrotest leakage indicates the presence of a through-wall defect, a detailed failure analysis was undertaken to determine the cause of crack initiation and propagation in the affected component. The submitted pipe section was made of AISI 316H austenitic stainless steel and had carbon steel studs joined by high-frequency resistance welding. Two leaks were reported in the tube under investigation, and one of the leaking regions was selected for detailed examination. The purpose of the investigation was to determine the crack morphology, verify the material chemistry, identify any microstructural anomalies or contamination, and establish the most probable root cause of the failure. The analytical approach combined surface inspection, chemical analysis, optical and stereomicroscopic examination, metallographic sectioning, and SEM/EDS investigation. These techniques were employed to characterize the crack path, identify the fracture mode, and assess whether the damage was associated with material non-conformance, welding-related discontinuities, or localized contamination introduced during fabrication.

2. Component Description and Fabrication History

The failed component was part of a convection module designed for heat recovery. The pipe material was identified as grade AISI 316H stainless steel. Carbon steel studs had been attached to the outer surface of the pipe by high-frequency resistance welding. According to the source report, the welding operation reportedly involved tools containing copper parts, which later became significant in the interpretation of the failure mechanism. During hydrotesting prior to commissioning, two leaks were detected in the investigated pipe. A section containing one of the leaking areas was cut from the component and submitted for failure analysis. The leaked region was marked on the received sample, and the selected portion was subsequently sectioned for detailed examination by metallography and SEM/EDS (Figure 1).

Figure 1: Studded pipe sample, as received

3. Failure Event and Hydrotest Observation

The failure was identified during hydrotesting carried out before commissioning. Two leak locations were found in the tube under investigation. One leaking location was selected for detailed examination in order to determine the mechanism responsible for crack formation and leakage. Since the failure occurred prior to service exposure, the observed cracking was considered to be associated with fabrication or pre-service processing rather than long-term operational degradation [2]. This is an important aspect of the case because it places emphasis on manufacturing-induced metallurgical damage as the probable origin of the failure.

4. Materials and Methods

4.1 Visual Examination and Dye Penetrant Inspection

Before sectioning, the internal surface of the pipe was cleaned and then subjected to dye penetrant inspection. The penetrant test confirmed the presence of one surface-breaking indication in the investigated region. The indication was linear in morphology and consistent with a longitudinal crack. In addition, the pipe exhibited localized bulging along circumferential regions near the crack location (Figure 2 & 3).

Figure 2: Pipe sample with dye penetrant inspection

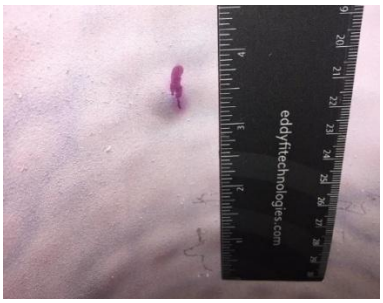

Figure 3: Condition of the pipe internal surface

4.2 Chemical Analysis

Optical emission spectroscopy was performed on a sample cut from the pipe section. The measured composition was compared with the nominal chemical composition for AISI 316H stainless steel. The reported results were 0.04% C, 0.40% Si, 0.89% Mn, 0.002% S, 0.035% P, 16.3% Cr, 11.1% Ni, 2.8% Mo, 0.16% Co, 0.29% Cu, and 0.063% N, which were considered consistent with the specified grade (Table 1).

Table 1: Chemical analysis results [%wt.]

	%C	%Si	%M	%S	%P	%Cr	%Ni	%M	%C	%C	%N
Grade AISI 316H nominal composition [2]	0.04-0.10	1.00	2.00	0.030	0.045	16.0-18.0	10.0-14.0	2.0-3.0	-	-	-
Lab Check Test Results	0.04	0.40	0.89	0.002	0.035	16.3	11.1	2.8	0.16	0.29	0.063

4.3 Visual and Stereomicroscopic Examination

The external and internal surfaces of the selected sample were visually examined, and the crack location was identified on both sides. The internal surface of the pipe exhibited heat tint. Close-

up examination by stereomicroscopy showed that the crack path on the internal surface had a morphology consistent with intergranular cracking. Part of the crack was forcibly opened to allow stereo and SEM fractography, while the remaining section was retained for metallographic examination in the transverse direction. Two views of the crack path, with respect to the stud positioning and weld region, were investigated to understand crack propagation (Figure 4a & 4b).

Figure 4: Crack location on the external (a) and internal (b) surface.

A general view of both sides of the sample, selected for further investigation, is shown in figure 4. In detail, the crack location is marked in figure 4a and 4b for the external and internal surface, respectively. As evident in figure 4b, the pipe surface exhibits heat tints (Figure 5 & 6).

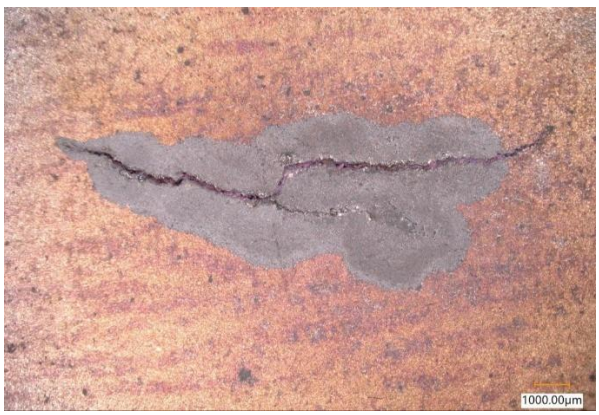

Figure 5: Additional close-up locations on the internal surface, x7.

Figure 6: Additional close-up on the internal surface, x70.

A general view of the crack path, as better visible by stereomicroscopy, is shown in figure 5 and 6 close-up view of the crack. As shown in the close-ups below, the internal surface exhibits an intergranular pattern (Figure 7 & 8).

Figure 7: Cutting plan for micro sectioning.

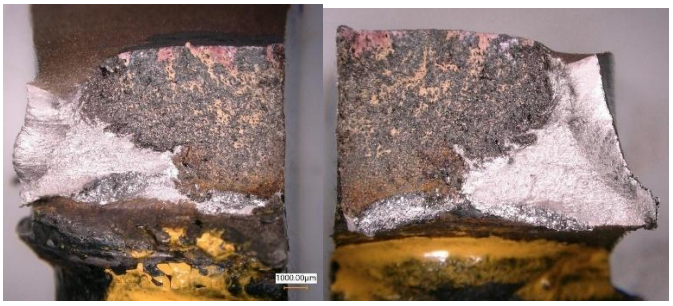

Figure 8: Matching fracture surfaces.

Micro sectioning was carried out as illustrated in figure 7. As visible below, the right portion of the crack was forced open to allow stereo and SEM fractography (figure 8). The remaining part of the crack was used for metallographic examination along the transverse direction. Two views of the crack propagation path, with respect to the stud positioning and welded joint was investigated for crack propagation pattern to study.

4.4 Metallographic Examination

A representative microsection from the cracked region was prepared and examined before and after etching. The selected cross-section was taken transverse to the leak and was intended to show the relationship between the crack path, the pipe wall thickness, and the stud attachment area. Additional micrographs were recorded to assess crack morphology and the condition of the surrounding microstructure. An additional microsection was also cut from a region away from the leaking area. This was done to determine whether similar cracking or contamination features were present elsewhere in the sample. A general view of the selected area is visible in figure 8 where the regions subjected to observation are illustrated. As evident below, the main crack path runs transversally through the pipe wall thickness with one end located at the lack of fusion between the right stud and the pipe external surface (figures 9 and 10b). Additional micrographs of the cracked area are verified prior and post etching respectively. Based on the metallographic evidence, the crack path appears to be predominantly intergranular in nature. Presence of a copperish-coloured matter was also observed along the crack internal surfaces (Figure 9 & 10).

Figure 9: Contact area between the stud and the pipe

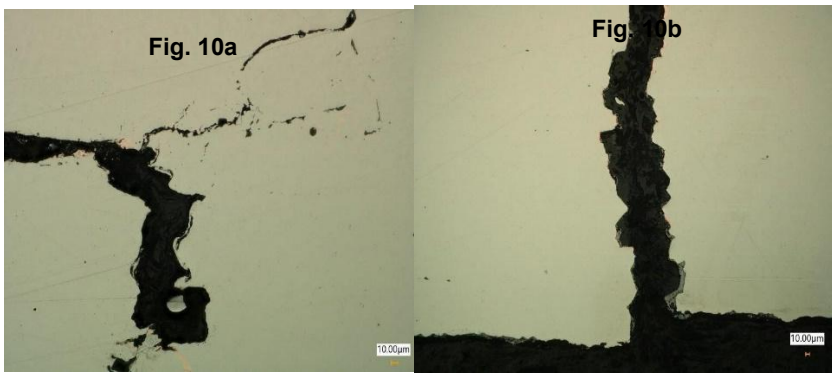

Figure 10: Cracked area condition prior etching.

5. Results

5.1 Macroscopic Features and Surface Condition

Visual examination and dye penetrant inspection confirmed the presence of a longitudinal, surface-breaking crack at the leaking location. The crack was associated with localized bulging in nearby circumferential regions. These observations indicated localized mechanical or thermal damage in the region rather than generalized degradation of the entire pipe wall. The internal pipe surface also exhibited heat tint near the damaged area. The presence of heat tint, together with the observed bulging, suggested that the region had experienced a localized thermal excursion during fabrication or processing.

5.2 Bulk Chemical Composition

The OES results showed that the bulk chemical composition of the pipe was consistent with the nominal composition of AISI 316H stainless steel. No evidence of incorrect base material chemistry was identified. This finding supports the view that the failure did not arise from alloy substitution or bulk compositional non-conformance.

5.3 Crack Morphology

Stereomicroscopy of the crack surface showed that the crack path was predominantly intergranular. The morphology observed in close-up views was consistent with grain-boundary separation rather than trans granular tearing. This interpretation was later confirmed by metallographic and SEM examination.

5.4 Metallographic Findings

Metallographic examination of the section taken transverse to the leak showed that the main crack extended across the pipe wall thickness. One end of the crack was located at a lack-of-fusion region between the right stud and the external surface of the pipe. This observation is important because it associates the crack directly with the stud attachment zone. The crack path was found to be predominantly intergranular in nature. In addition, a copperish-colored matter was observed along the internal surfaces of the crack. The surrounding microstructure of the pipe was considered consistent with the expected condition of the austenitic grade under investigation.

6. Discussion

The combined observations indicate that the investigated failure was caused by a localized cracking mechanism rather than by bulk material non-conformance. The OES results

confirmed that the pipe chemistry was consistent with AISI 316H, and the metallographic observations showed that the microstructure of the pipe was consistent with the expected condition of the austenitic alloy. Accordingly, the failure cannot be attributed to an incorrect base material. The crack was longitudinal, through-wall, and predominantly intergranular in morphology. This conclusion was consistently supported by dye penetrant inspection, stereomicroscopy, metallographic examination, and SEM fractography. The fracture path indicates intergranular decohesion rather than transgranular fracture or ductile overload. One of the most significant findings of the investigation was the repeated observation of copper along the crack path. Copperish-colored matter was first observed optically, and confirmed the presence of copper on both the opened fracture surface and the internal crack surfaces in cross-section. This direct association between intergranular fracture and localized copper presence led to the interpretation that the failure was consistent with liquid metal embrittlement of austenitic stainless steel by copper [1]. The fabrication context given in the source document supports this interpretation. The report states that the welding operation reportedly involved tools containing copper parts and that the welding process may have provided temperatures high enough for the detrimental mechanism to occur. Localized bulging and heat tint observed in the damaged region further support the possibility of local overheating during the stud welding stage. Metallography also showed that one end of the crack was located at a lack-of-fusion region between the stud and the external pipe surface. This observation places the crack in direct association with a local fabrication discontinuity and strengthens the view that the failure originated during or in connection with the stud welding operation. The additional analyses performed away from the main leaking area suggest that copper contamination was localized rather than generally distributed throughout the sample. Although another crack was found in a secondary region, copper was not detected in the three additional analysed areas. Instead, those areas showed oxygen, carbon, or silicon, with silicon likely attributable to preparation consumables. This contrast supports the conclusion that the principal failure involved a localized copper-assisted embrittlement event.

7. Root Cause Assessment

Based on the results of the investigation, the root cause of the cracking issue affecting the submitted pipe sample was identified as copper contamination of the austenitic stainless steel in the failed region, resulting in intergranular embrittlement. Metallographic examination, SEM fractography, and EDS analysis all demonstrated a predominantly intergranular crack path with copper present along the fracture and crack surfaces [3]. This combination of findings was

considered consistent with liquid metal embrittlement of austenitic stainless steel by copper. The fabrication stage most strongly implicated by the observations was the stud welding operation. The source report notes that copper-containing tooling was reportedly involved during welding and that sufficient local temperature may have been generated for this mechanism to occur. The observed heat tint, bulging, and lack of fusion near the stud/pipe interface provide further support for the conclusion that fabrication-related overheating and copper contamination played a key role in crack initiation and propagation [4-10].

9. Conclusions

1. The bulk chemical composition of the failed pipe was consistent with the nominal composition of AISI 316H stainless steel.
2. Dye penetrant inspection revealed a linear surface-breaking indication consistent with a longitudinal crack.
3. Localized bulging and heat tint were observed in the damaged region, indicating possible local overheating.
4. Stereomicroscopy and metallographic examination showed that the main crack propagated through the wall thickness and was predominantly intergranular in nature.
5. One end of the crack was associated with a lack-of-fusion region between the stud and the external surface of the pipe.
6. SEM fractography confirmed the intergranular character of the fracture and the brittle nature of the cracking mechanism.
7. Copper-rich matter was observed along the crack path and was confirmed by EDS on both the opened fracture surface and the internal crack surfaces in cross-section.
8. The overall failure mechanism was considered consistent with copper-induced liquid metal embrittlement of the austenitic stainless steel during the stud welding stage under conditions of elevated local temperature.
9. Further investigation into the origin and transfer mode of copper contamination was strongly recommended.

10. References

1. Rao, S., and Al-Kawaie, A.Y. Copper Contamination Cracking in Austenitic Stainless Steel Welds. Welding Journal, 89, 46–49 (2010).

2. Norkett, J.E., Dickey, M.D., and Miller, V.M. A Review of Liquid Metal Embrittlement: Cracking Open the Disparate Mechanisms. Metallurgical and Materials Transactions A, 52, 2158–2172 (2021). DOI: 10.1007/s11661-021-06256-y.
3. Bejugama, S., Manigandan, S., Raju, V., Eggidi, O. Failure Analysis of Austenitic Stainless Steel Weldments: The Role of Copper Contamination and Crack Propagation Mechanisms. Journal of Failure Analysis and Prevention. 2025;25:1408–1415. https://doi.org/10.1007/s11668-025-02218-3
4. Sun, Z., Li, P., Zhang, T., Wang, J., Xu, D., Chen, H., Liu, D., Pei, Y. Effect of Stress and Si on Liquid Metal Embrittlement of 316L(N)-Copper. Materials Science and Technology. 2021;37(5):552–559. https://doi.org/10.1080/02670836.2021.1929718
5. ASM Metals Handbook, Vol. 1: Properties and Selection of Irons, Steels and High-Performance Alloys.
6. Zhang X, et al. Surface-enhanced Raman spectroscopy for the detection of organic pollutants in water: A review. TrAC Trends Anal Chem. 2021;136:116246.
7. Cieplak M, Kutner W. Molecularly imprinted polymer-based sensors for biomedical and environmental applications. Anal Chim Acta. 2016;935:1–27.
8. A corrosion failure analysis of heat exchanger tubes operating in petrochemical refinery. Eng Fail Anal. 2021;119:105011.
9. Degradation of stainless steel grids in chemically aggressive environment. Eng Fail Anal. 2013;35:418–426.
10. Corrosion of stainless steels in the riser during co-processing of bio-oils in a fluid catalytic cracking pilot plant. Fuel Process Technol. 2017;159:187–199.